Chin. Geogra. Sci. 2024 Vol. 34 No. 1 pp. 106−117
https://doi.org/10.1007/s11769-024-1411-3

Springer Science Press
www.springerlink.com/content/1002-0063

Monitoring Surface Water Change in Northeast China in 1999–2020: Evidence from Satellite Observation and Refined Classification

LIU Kai[1, 2], ZHANG Dapeng[3], CHEN Tan[1], CUI Peipei[1], FAN Chenyu[1, 2], SONG Chunqiao[1, 2]

(1. *Key Laboratory of Watershed Geographic Sciences*, *Nanjing Institute of Geography and Limnology*, *Chinese Academy of Sciences*, *Nanjing* 210008, *China*; 2. *University of Chinese Academy of Sciences*, *Nanjing* (*UCASNJ*), *Nanjing* 211135, *China*; 3. *Geographic Information and Tourism College*, *Chuzhou University*, *Chuzhou* 239000, *China*)

Abstract: As a typical region with high water demand for agricultural production, understanding the spatiotemporal surface water changes in Northeast China is critical for water resources management and sustainable development. However, the long-term variation characteristics of surface water of different water body types in Northeast China remain rarely explored. This study investigated how surface water bodies of different types (e.g., lake, reservoir, river, coastal aquaculture, marsh wetland, ephemeral water) changed during 1999–2020 in Northeast China based on various remote sensing-based datasets. The results showed that surface water in Northeast China grew dramatically in the past two decades, with an equivalent area increasing from 24 394 km^2 in 1999 to 34 595 km^2 in 2020. The surge of ephemeral water is the primary driver of surface water expansion, which could ascribe to shifted precipitation pattern. Marsh wetlands, rivers, and reservoirs experienced a similar trend, with an approximate 20% increase at the interdecadal scale. By contrast, coastal aquacultures and natural lakes remain relatively stable. This study is expected to provide a more comprehensive investigation of the surface water variability in Northeast China and has important practical significance for the scientific management of different types of surface water.

Keywords: surface water; spatiotemporal variation; water body classification; remote sensing; Northeast China

Citation: LIU Kai, ZHANG Dapeng, CHEN Tan, CUI Peipei, FAN Chenyu, SONG Chunqiao, 2024. Monitoring Surface Water Change in Northeast China in 1999–2020: Evidence from Satellite Observation and Refined Classification. *Chinese Geographical Science*, 34(1): 106−117. https://doi.org/10.1007/s11769-024-1411-3

1 Introduction

Surface water bodies, including rivers, lakes, reservoirs, wetlands, and some ephemeral waters (e.g., lagoons, floodplains, rice fields), are the most accessible water resource to human populations (Pekel et al., 2016; Zhang et al., 2023). Recent climate change and intensifying human activity have amplified the variability of surface water in both seasonality and persistence (Cooley et al., 2021). Practically, the rapid changes in surface water caused by extreme climate events are often accompanied by unprecedented floods and droughts, which severely impact ecosystems and threaten the security of people and economies (Tulbure et al., 2016; Christian et al., 2021). Therefore, accurately tracking and quantifying surface water dynamics will help us

Received date: 2023-01-10; accepted date: 2023-05-21

Foundation item: Under the auspices of Strategic Priority Research Program of the Chinese Academy of Sciences (No. XDA28020503, XDA23100102), National Key Research and Development Program of China (No. 2019YFA0607101), Project of China Geological Survey (No. DD20230505), Excellent Scientific Research and Innovation Team of Universities in Anhui Province (No. 2023AH010071)

Corresponding author: SONG Chunqiao. E-mail: cqsong@niglas.ac.cn

better understand the water cycle and protect water resource-related ecosystem services.

The development of remote sensing technology favors an effective approach for monitoring surface water dynamics at large scales. Satellites-based observation of surface water at an early stage relies on coarse-resolution satellite sensors such as National Oceanic Atmospheric Adminstration/Advanced Very High Resolution Radiometer (NOAA/AVHRR) (~1 km resolution) and Terra/Aqua MODerate-resolution Imaging Spectroradiometer (MODIS) (250 m to 1 km resolutions) (Sheng et al., 2016), they are limited only to large water bodies. After the free access to Landsat imagery in 2008 (30-m spatial resolution), the tracking of surface water dynamics has become feasible and affordable even at a global scale. Especially due to the advances in cloud computation featured by the popularity of the Google Earth Engine (GEE) platform, our knowledge of the distribution of and temporal changes in Earth's surface water has dramatically increased over the recent few years (Pekel et al., 2016; Weekley and Li, 2019; Zhou et al., 2019; Xu et al., 2022). The spatiotemporal variability of their water extents and driving factors have been investigated at vulnerable regions to global changes (Yang et al., 2017; Shugar et al., 2020; Gao et al., 2021; Luo et al., 2022; Pi et al., 2022; Zhou et al., 2022). However, previous studies mostly investigated the variations of various surface water bodies as aggregation or focused on one specific type, without an explicit differentiation and comparison of surface water dynamics in different types, such as lakes, reservoirs, and rivers. Currently, an increasing number of global water bodies datasets have been released, such as Hydrographic Lakes (HydroLAKES) (Messager et al., 2016), Georeferenced Global Dam And Reservoir (GeoDAR) (Wang et al., 2021), and Global River Widths from Landsat Database (GRWL) (Allen and Pavelsky, 2018), which provide the reference data for identifying variations of different water body types in different regions.

Northeast China is a famous granary featured by its fertile soil and widespread plains. The abundant surface water in this region is also essential for agriculture production and food security. Previous studies have indicated that the Earth's surface water in Northeast China is sensitive to climate change, for example, through heavy precipitation or rising temperature (Zhang Y et al., 2019; Du et al., 2020). Meanwhile, intensified human activities in this region may alter the surface water dynamic, especially by operating reservoir dams, reclamation, and agricultural irrigation (Wang et al., 2015). Although remote sensing-based monitoring of surface water has been conducted in this region ranging from an individual lake to basin-scale assessment (Yu et al., 2018; Yan and Zhang, 2019; Fan et al., 2021), the incomplete information about water cover types limits the knowledge of different changing pattern of each water bodies (Shan et al., 2022). A comprehensive study focusing on how multiple water-covered bodies have changed, impacted by climate change and human activities, is thus urgently needed for effective utilization of water resources in Northeast China.

The aim of this study is to monitor how different types of water body changes during 1999–2020 in Northeast China. The objectives of this study are as follows: 1) to classify surface water types in Northeast China by integrating multi-source remote sensing data; 2) to evaluate the overall distribution characteristics of surface water in Northeast China in the year 2020; 3) to reveal the spatial and temporal variation of different types of surface water in Northeast China at the interdecadal and interannual scales, and to analyze their correlation with climate change and human activities. This study is expected to provide a scientific reference for water resource management in Northeast China.

2 Materials and Methods

2.1 Study area

Northeast China covers Heilongjiang, Jilin, and Liaoning provinces as well as Hulunbuir, Tongliao, Chifeng cities, and Hinggan League of the Inner Mongolia Autonomous Region, with an area of about 1.25 million km^2. Northeast China has a temperate monsoon climate, with a topographic pattern of surrounding mountains and internal plains. The humid climate and diverse topography have created relatively rich surface water resources (Fig. 1). The major rivers are the Songhua River, Nenjiang River, Liaohe River, Heilong River, Wusuli River, Tumen River, and Yalu River. The typical large lakes include Hulun Lake, Chagan Lake, and Lianhuan Lake. Furthermore, the study region is China's main distribution area of wetlands (Mao et al., 2020). Although the total water resource in Northeast China is abundant, the water stress is still severe in this region from the per-

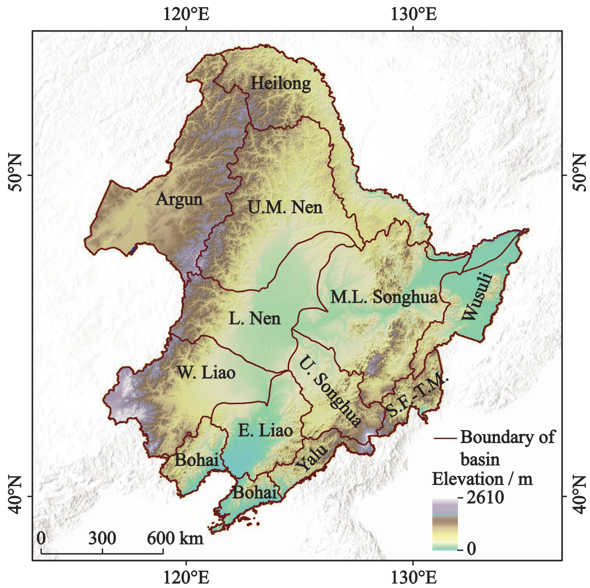

Fig. 1 Location of Northeast China and spatial distribution of the watershed units in the study area. Argun River Basin (Argun), Heilong River Basin (Heilong), Upper and Middle Nenjiang River Basin (U.M. Nen), Lower Nenjiang River Basin (L. Nen), Middle and Lower Songhua River Basin (M.L. Songhua), Upper Songhua River Basin (U. Songhua), Wusuli River Basin (Wusuli), Suifen River and Tumen River Basin (S.F.-T.M.), West Liaohe River Basin (W. Liao), East Liaohe River Basin (E. Liao), Yalu River Basin (Yalu), and Bohai Bay Basin (Bohai)

spective of social and economic development demands. As an area with a high level of urbanization and industrialization, the contradiction between the supply and demand of water resources is very prominent. In addition, the study region is the most crucial grain production base and commodity grain export base in China. Therefore, crop cultivation has a great demand for water resources, and monitoring and efficient use of water resources is essential to ensure grain production in Northeast China (Wang et al., 2018).

The secondary watershed units were adopted for further statistics to reveal the spatial pattern of the surface water in the study area (http://lake.geodata.cn). There are 12 units, including Argun River Basin (Argun), Heilong River Basin (Heilong), Upper and Middle Nenjiang River Basin (U.M. Nen), Lower Nenjiang River Basin (L. Nen), Middle and Lower Songhua River Basin (M.L. Songhua), Upper Songhua River Basin (U. Songhua), Wusuli River Basin (Wusuli), Suifen River and Tumen River Basin (S.F.-T.M.), West Liaohe River Basin (W. Liao), East Liaohe River Basin (E. Liao), Yalu River Basin (Yalu), and Bohai Bay Basin (Bohai) (Fig. 1).

2.2 Data

2.2.1 Global surface water dynamic data

Remote sensing data allow rapid tracking of long-term and large-scale surface water change. Compared with surface water mapping based on imagery by using different water indexes, the availability of global surface water occurrence maps provided by the Joint Research Centre (JRC) and Global Land Analysis and Discovery (GLAD) lab makes the long-term monitoring of water dynamics more flexible (Pekel et al., 2016; Pickens et al., 2020). This study adopted the GLAD Global Surface Water Dynamic (GSWD) data due to its potential advantages in mapping small water bodies (Pickens et al., 2022). Long-term and high-frequency global land and surface water classification in the GLAD GSWD dataset were achieved by combining Landsat 5, 7, and 8 data. Based on the water classification for all available imagery, the dataset provides year-by-year and month-by-month water occurrence frequency data since 1999, which records the probability that each grid is a type of water over a specific period. When the water occurrence frequency equals 100, all observations within a given period are identified as water. When the water occurrence frequency is 0, the pixel is not water in all observations. In this study, we generated the surface water extents during the study periods based on the annual water occurrence layer from GLAD GSWD data.

2.2.2 Reference data for water type classification

Although the GLAD GSWD data can indicate the probability of water presence, it can not directly classify different water body types. According to the existing water body classification system and the regional features of the study area, a total of six categories needed to be classified, including lakes, reservoirs, rivers, marsh wetlands, coastal aquacultures, and ephemeral waters. We employed national-scale lake and reservoir datasets produced by our previous studies as a reference, including the Maximum Water Extent of Chinese Lakes (MWECL) (1984–2018) and the China Reservoir Dataset (CRD) (Song et al., 2022; Zhang and Song, 2022). The reference data for determining river extent are from the Global River Widths from Landsat (GRWL) dataset (Allen and Pavelsky, 2018). In addition, to distinguish between marsh wetlands and other water bodies, we used the global land-cover data GLC_FCS30 with a spatial resolution of 30 m (Zhang et al., 2021). The distribution of wetlands derived from GLC_FCS30 is regarded as a reference in water body classification. The high-resolution imagery provided by ArcGIS online was also adopted as a supplement for manual interpretation.

2.3 Methods

2.3.1 Surface water extraction and equivalent area calculation

This study mainly used the water occurrence frequency provided by GLAD GSWD data to extract the water extent. We utilized the annual history product of GLAD GSWD, which records the average annual percentage of time for which water was present. Within a 20-yr period from 1999 to 2020, the union of all pixels greater than zero in the GLAD GSWD annual product was taken and referred to as multi-year maximum water extent. Multi-year maximum water extent provides spatial constraints for subsequent water classification and dynamic water analysis. To track the interannual water dynamic, permanent and maximum water extent were easily detected by setting the frequency to 100 and greater than 0, respectively. To accurately quantify the surface water dynamic, we also introduced the concept of equivalent water area: the water occurrence frequency multiplied by the corresponding flooded area, that is, the accumulation of the flooded frequency of all observed pixels in a certain period of time. The interannual water occurrence frequency formula is given by:

$$AWF = \frac{AOWT}{AOT} \tag{1}$$

where annual water frequency (*AWF*) is the interannual water occurrence frequency, annual observed water time (*AOWT*) represents the number of times water appears in the pixel during the year, and annual observation time (*AOT*) represents the number of valid observations for the pixel in the year. Based on the annual water occurrence frequency in each pixel, the annual equivalent water area of surface water was calculated. The equivalent water area (*EWA*) formula is as follows:

$$EWA = \sum_{i=1}^{n} AWF \times PA_i \tag{2}$$

where PA_i is the area of pixel *i*. *n* is the total number of pixels. We calculated the equivalent water area (EWA) for each pixel by multiplying *AWF* and *PA*. *EWA* considers the weights of water occurrence frequency, which may be less sensitive to extreme flooding events. By contrast, water maximum area based on simple pixel counting does not distinguish between permanent and ephemeral water bodies. It is believed that *EWA* is more robust and reasonable for monitoring the inter-annual and intra-annual characteristics of each lake (Zhang and Song, 2022). In this study, *EWA* was used to calculate the water extent dynamic in Northeast China from 1999 to 2020.

2.3.2 Surface water classification

The basic assumption of water classification in this study was that there was no large-scale water-type conversion during the study period. Hence, the water type classification based on multi-year maximum water extent can support the following interdecadal and interannual analysis. According to the importance of different water types, this study determined the spatial extent of six types of surface water in the order of lakes, reservoirs, rivers, coastal aquaculture, marsh wetlands, and ephemeral waters (Fig. 2). The referenced lakes and reservoirs extents were determined based on adopted lake and reservoir inventories, i.e., MWECL and CRD. In total, there are 780 lakes and 243 reservoirs greater than 1 km^2 in Northeast China. As for each lake or reservoir, we updated the maximum water extent by the following steps. First, a buffer zone was set to determine the potential expanded area of the selected lake or reservoir. For lakes and reservoirs with an area greater than 100, 10–100, and an area less than 10 km^2, the sizes of the buffer zones were set to 1 km, 500 m, and 300 m, respectively. Second, the spatial relationship between all water bodies in the buffer zone and the reference data was interpreted. If the water bodies intersected with the reference lake or reservoir, it could be considered as its expansion area and was retained. Finally, by combining all the reserved water bodies, the maximum water extent of the selected lake or reservoir could be updated. A similar approach was used to determine the maximum extent of river water. The difference is that the reference data of rivers are linear features; hence, a much larger buffer size was needed. For the river segments with the stream order of 1, 2, and less than or equal to 3, the buffer zone was set to 10, 5, and 3 km, respectively. When judging whether the potential water bodies within the buffer zone were a river, manual judgment based on the high-resolution imagery was adopted. The manual visual interpretation was also conducted to determine the coastal aquaculture areas because of the relatively clear distribution along the coastal lines. The maximum water extent of the marsh wet-

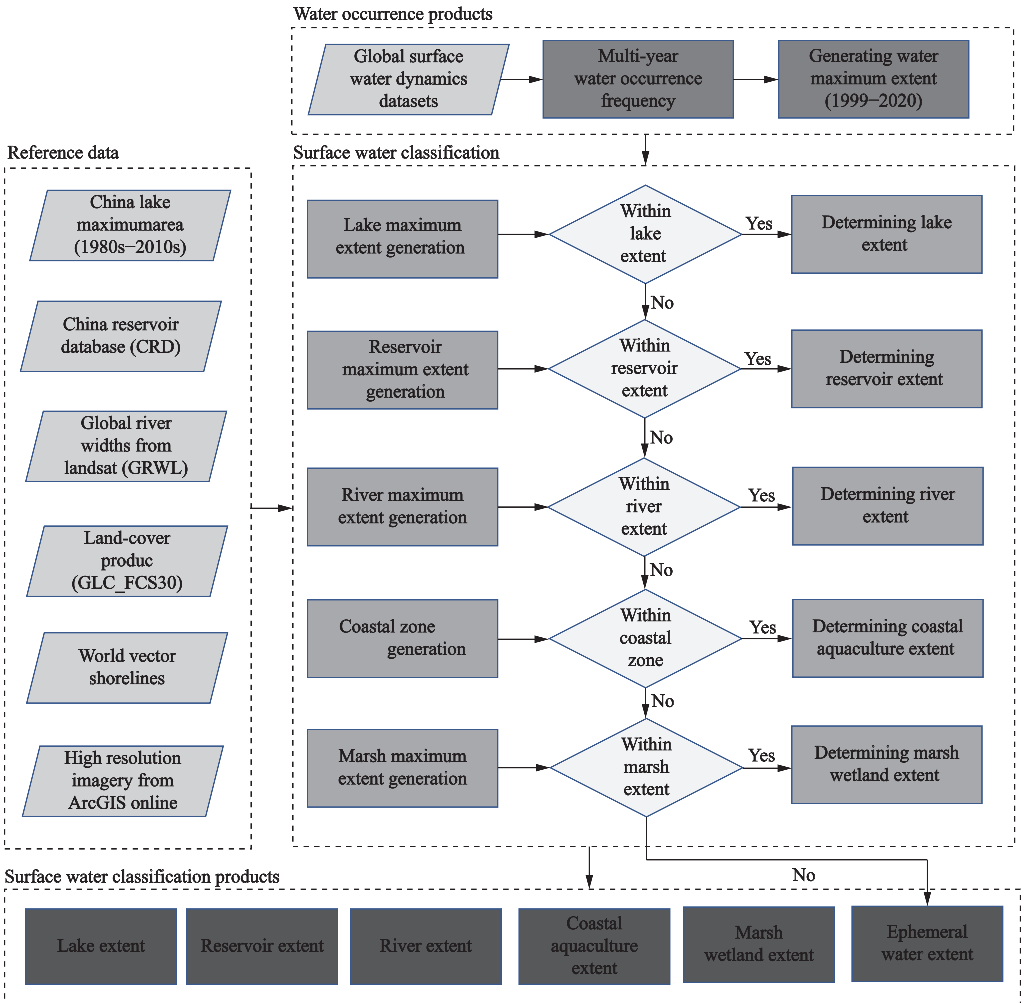

Fig. 2 Workflow for water body classification

land was based on the land-use data every five years from 2000 to 2020. After merging the multi-period wetland extents derived from GLC_FCS30, the remaining water bodies (removal of classified lakes, reservoirs, rivers, and coastal aquaculture) within the merged wetlands extents were labeled as marsh wetlands. By categorizing the above five types of water bodies, the remaining water bodies were all marked as ephemeral waters. Ephemeral water is water that occurs less frequently within a year, including flood plains, paddy fields, grasslands, and impervious layers. The classified water bodies based on multi-year maximum water extents (1999–2020) are illustrated in Fig. 3.

3 Results and Analyses

3.1 Spatial distribution of surface water in Northeast China in 2020

The equivalent surface water area in Northeast China in 2020 is about 34 595 km^2, of which the seasonal water is 20 297 km^2, and the permanent water area is 14 298 km^2. The seasonal water area is slightly larger than the permanent water area. As shown in Fig. 4, there are three peaks of surface water in the east-west direction. Hulun Lake mainly dominates the high-value area in the west. Chagan Lake, Lianhuan Lake, and the widespread marsh wetlands and rivers primarily dominate the high-value area in the central Songnen Plain. The Sanjiang Plain is also a region with high water density, where Xingkai Lake and many ephemeral water bodies are distributed. The distribution pattern of water in the north-south direction is relatively clear. The peak value mainly occurs in the range of 45°N–47°N, primarily contributed by the Songnen Plain and the Sanjiang Plain. By contrast, fewer water bodies are distributed north of 50°N and south of 45°N.

After revealing the distribution pattern of surface wa-

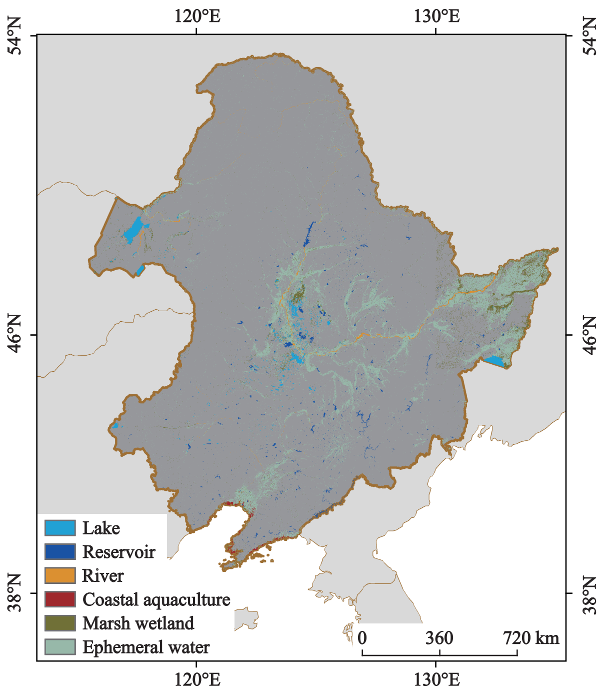

Fig. 3 Water bodies classification results based on multi-year water maximum extent in Northeast China from 2000 to 2020. The grey background in the study area represents non-water area

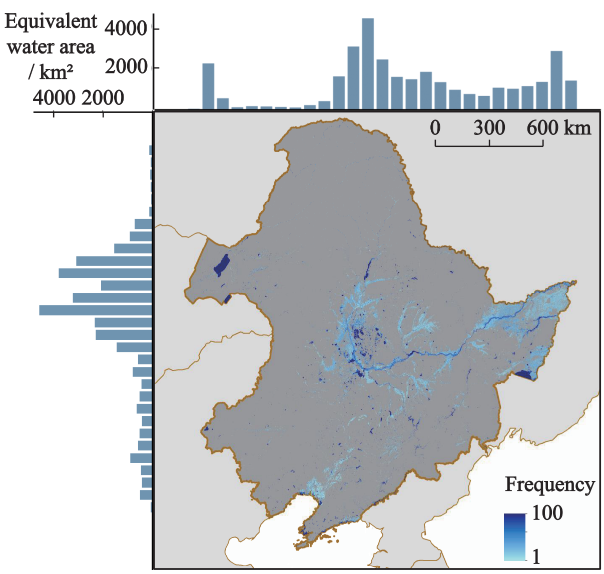

Fig. 4 Spatial distribution of the water occurrence frequency in Northeast China in 2020. The grey background in the study area represents non-water area. The top and right histograms reflect surface water distributions in longitude and latitude directions

ter in Northeast China in 2020, this study further classified surface water into six types. As shown in Table 1, the equivalent water area of ephemeral water is the largest in 2020, accounting for 44.02% of the total surface water area in Northeast China. The ephemeral water is dominated by seasonal water, with an area of 13 420 km^2, 7.42 times of that for the permanent water (1809 km^2). This also suggests that although ephemeral water has a wide distribution area, it fluctuates significantly during the year. The equivalent area of lake extent ranks second, with an area of 6592 km^2. Among lake water bodies, the permanent water is 5616 km^2, accounting for 72.02% of the maximum area. The equivalent water area of ephemeral water is more than twice that of lakes; however, its permanent water area is only 32.21% of lake-type water bodies. The coastal aquacultures occupy the smallest area, with an equivalent water area of 973 km^2. More statistics of surface water distribution in different secondary basin units is provided in Table S1.

3.2 Interdecadal variation of surface water in Northeast China

We analyzed the spatiotemporal variability of surface water in Northeast China since 1999 on both interdecadal and interannual scales. The interdecadal variation was calculated based on the average equivalent surface water area in the two time periods, 1999–2009 and 2010–2020 (Fig. 5). During the two periods, the surface water area in Northeast China increased by 9561 km^2 (43.41%). Among the six types of surface water, only the areas of the lake and coastal aquaculture remain stable, while the areas of other types increase significantly. The equivalent area of ephemeral water type increases by 7161 km^2, accounting for 74.90% of the total water change. The rapid increase of this type is the main factor for the surface changes in Northeast China on the interdecadal scale. In addition, marsh wetlands also expanded dramatically, with an increased ratio of 37.36% (Table S2).

3.3 Annual variation of surface water in Northeast China

To precisely reveal the variation of surface water in Northeast China, we analyze the equivalent area changes of various types of surface water on an interannual scale (Fig. 6). The results show that since 1999, the surface water in Northeast China has shown a gradual decline at first before 2002, then stability, and then a rapid rise after 2010. Here we compare the first and last years of the study period (Table S3). A noticeable expansion of

Table 1 Area statistics of different types of water bodies in Northeast China in 2020 / km^2

Water type	Lake	Reservoir	River	Marsh wetland	Coastal aquaculture	Ephemeral water
Seasonal water	976	1546	696	3245	414	13420
Permanent water	5616	3970	1085	1259	559	1809
Maximum area	7797	6834	2902	10411	1325	68215
Equivalent area	6592	5516	1781	4504	973	15229

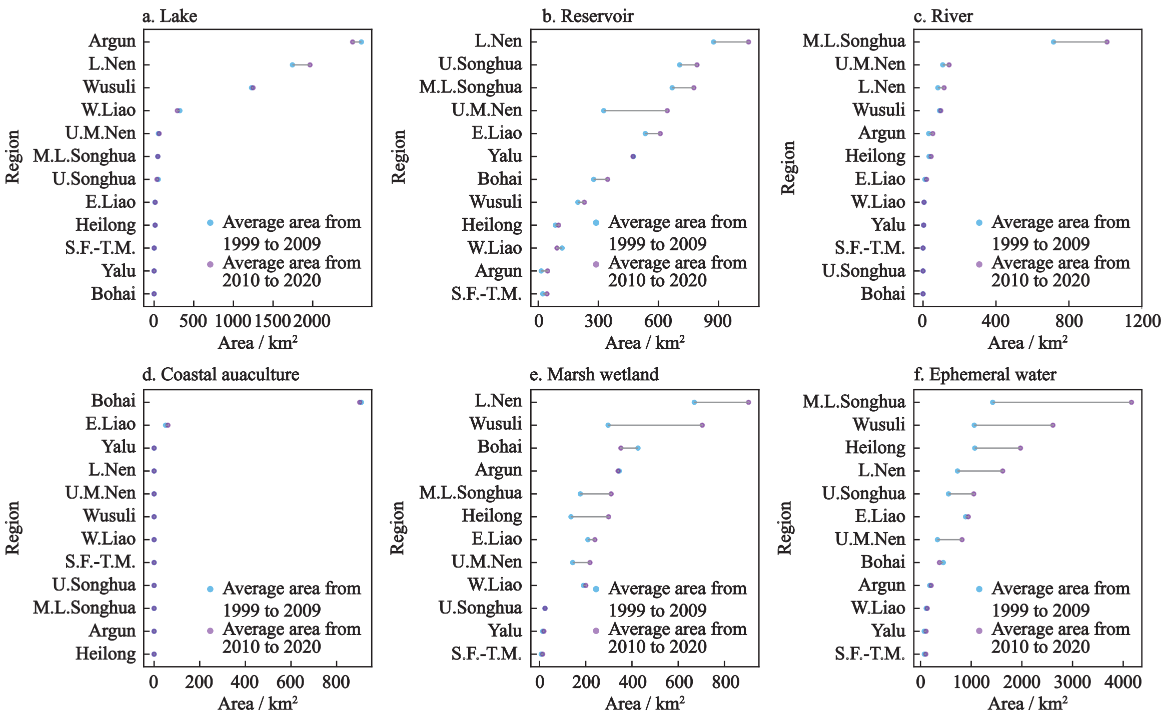

Fig. 5 Equivalent water area changes of different kinds of water bodies between 1999–2009 and 2010–2020. Watershed names are shown in Fig. 1

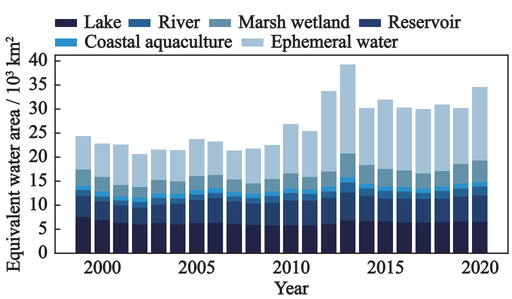

Fig. 6 Annual equivalent water area of six water body types in Northeast China during 1999–2020

surface water has been observed in Northeast China in the past two decades, with an equivalent area increase of 41.82%. Among them, the area of permanent water is relatively stable, with an increase of 4.92% (671 km^2). By contrast, seasonal water increases by 88.51% (9530 km^2). From 1999 to 2020, seasonal and permanent water proportions changed from 44.14% and 55.86% to 58.67% and 41.33%, respectively. It suggests that seasonal water gradually becomes the dominant part of surface water in Northeast China.

We further examine the variation trends of different kinds of water bodies. Permanent water dominates lakes, reservoirs, and rivers. By contrast, seasonal water occupies large proration of the total area in marsh wetlands and ephemeral waters (Fig. 7). The calculated change ratios indicate that only lakes experienced a general decline in the past two decades, with the equivalent area dropping from 7598 to 6592 km^2. The increased ratios of coastal aquacultures, reservoirs, marsh wetlands and rivers are 10.69%, 27.48%, 30.21%, and 42.94%, respectively. Particular emphasis should be paid to the dramatic increase of ephemeral water. The equivalent area of ephemeral water in 1999 was only 6885 km^2,

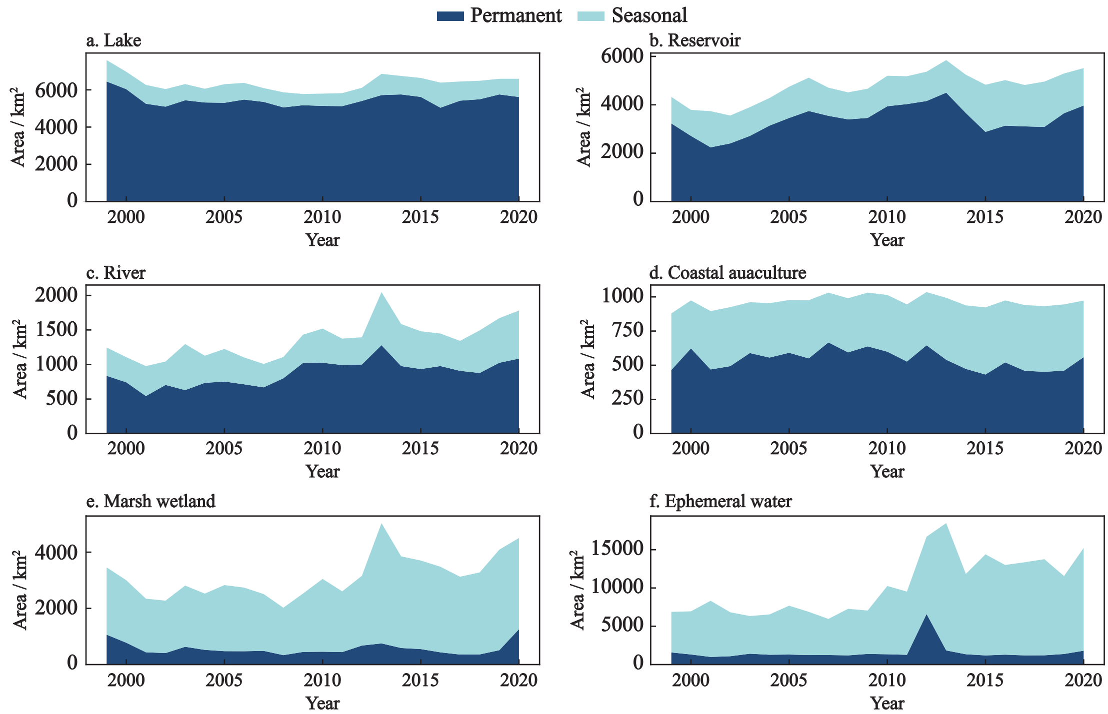

Fig. 7 Annual variation of different types of water bodies by separating permanent water and seasonal water in Northeast China during 1999–2020

even smaller than the lakes' area. By contrast, the ephemeral water in 2020 took up an area of 15 229 km^2, increasing by 121.19%.

It should be noted that the equivalent area in 2002 was 20 671 km^2, only 52.65% of the maximum value achieved in 2013. A further comparison analysis was conducted to detect the potential drivers of anomalous years (Fig. 8). Comparisons between 1999 and 2002 show that the shrinkage of lakes, reservoirs, and marsh wetlands led to the rapid decline in 2002. The changes ratios are −20.49%, −17.81%, and −34.23% for the above three water types (Table S3). Since the turning point in 2002, surface water in Northeast China experienced an overall increasing trend until achieving the maximum point in 2013. Between 2002 and 2013, lakes, reservoirs, rivers, and marsh wetlands all expanded. Especially for marsh wetlands, the equivalent area increases from 2275 to 5035 km^2. However, ephemeral water was the leading contributor to the sharp growth in surface water in 2013. The equivalent area of ephemeral water in 2013 reached 18 475 km^2, which is close to three times that in 2002. A further discussion of the underlying drivers of the divergent change trends in different periods will be conducted in Section 4.2.

4 Discussion

4.1 Uncertainty analysis

The uncertainty of the analysis here was mainly from two aspects: the water body extraction and water body classification. In the existing surface water dynamic studies, a standard for data selection has usually been determined at first. Then the water extent was extracted based on the optical image data (such as Landsat or Sentinel) that met the conditions in different periods. For example, when Zhang et al. conducted a national-scale lake dynamic change study, the images with few clouds in October were prioritized (Zhang G Q et al., 2019). Nevertheless, some scholars believe that representing the whole year's results by a single moment water extent of the year introduces some uncertainty. Particularly for lakesindifferentclimaticregions,themonthswhentheyreach the wet season are different, directly affecting the area comparability between various lakes. For this reason, some studies have selected all available Landsat images in the year to extract the water extent (Zou et al., 2017). The water occurrence frequency in each grid was calculated to generate a water occurrence frequency map. Finally, different water occurrence frequency thresholds were set to determine the water extent of wet, dry, and

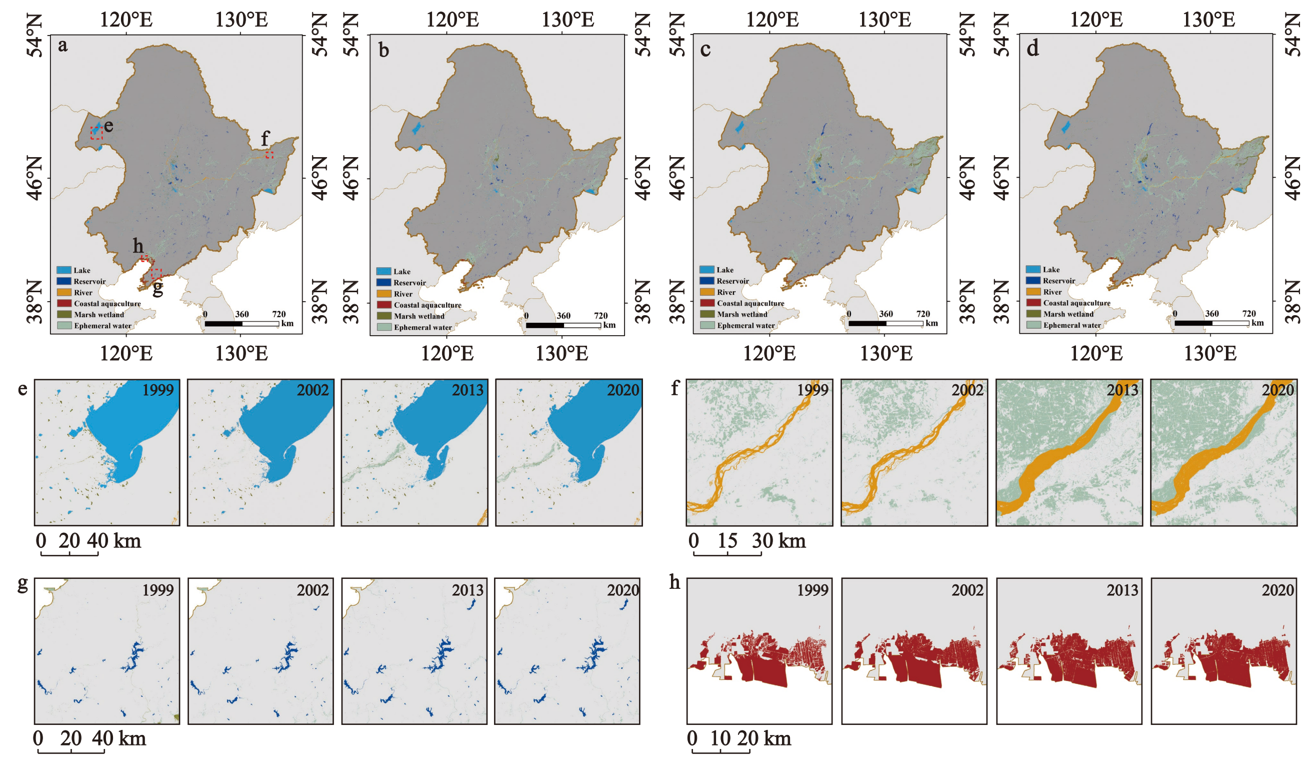

Fig. 8 Classified water bodies in four specific years, including (a) starting year (1999), (b) year with the minimum area (2002), (c) year with the maximum area (2013), and (d) ending year (2020) in Northeast China. Four enlarged regions mainly focus on water dynamics of (e) lakes, (f) rivers and ephemeral water, (g) reservoirs, and (h) coastal aquaculture

regular seasons during the year. This method can avoid abnormal fluctuations when extracting water extent from a single image at the moment. This study also adopted the idea of extracting water extent from the water occurrence frequency data. The difference is that we directly applied the annual water occurrence frequency data from the shared GLAD GSWD dataset. As a result, the data can accurately distinguish between pure land and pure water pixels (with an average accuracy of more than 95%). The extraction error is mainly due to the interference of mixed pixels, the land-water boundary. The accuracy analysis results of GLAD GSWD data show that the correct classification accuracy of water pixels at the land-water boundary could reach about 70%.

The uncertainty of water classification mainly came from the simplified method adopted in this study. We assumed there was no conversion between different types of surface water, and the analysis of surface water changes year by year was achieved by classifying the types of the maximum water extent of surface water. In practice, a small amount of type conversion between water bodies also exists. For instance, a newly impounded reservoir causes river water to be transformed into a reservoir. According to the classification method of this study, the water in the reservoir area before its impoundment would be misclassified. Moreover, this study's area threshold of the lake reference data was 1 km^2. Small lakes less than 1 km^2 are classified as temporary water. However, in general, the uncertainty of the above classification has little effect on the results of the overall trend analysis.

Six sample sites with varying dominant water body types were chosen in order to validate the accuracy of surface water classification (Fig. S1). For each sample area, 1000 random points were created, and high-resolution imagery from ArcGIS Online (DigitalGlobe, ac-

Table 2 Accuracy statistics for classification of six typical water body in Northeast China during 1999–2020

Accuracy	Lake	Reservoir	River	Marshwetland	Coastal aquaculture	Ephemeral water
Overall accuracy / %	98.60	97.50	98.10	96.90	98.70	99.10
Kappa coefficient	0.97	0.86	0.92	0.87	0.97	0.95

quired in May 2020) was used to undertake visual interpretation. After generating the referenced data manually, the classification accuracy for each area was calculated by comparison with the annual 2020 results. Table 2 demonstrates that all six areas have overall accuracies that are greater than 96%. Ephemeral water area achieves the highest accuracy (99.10%). By contrast, the performance in the marsh wetland region is relatively poor, with an overall accuracy of 96.90%.

It should also be noted that the definition of water bodies could bring different results than previous studies. For example, the definition of wetland in this study is limited to the inland marsh. By contrast, lakes, rivers, and human-made water bodies such as reservoirs and paddy fields all belong to the wetland in the CAS_Wetlands system (Mao et al., 2020). The small distribution of wetlands in this study was caused by the strict definition instead of omission errors.

4.2 Analysis of driving factors

Our results have demonstrated that the surface water area in Northeast China has generally increased since 1999, and there are abnormally two high values in 2013 and 2020. Previous study have pointed out the predominant role of climate change in surface water dynamics (Pekel et al., 2016). This study collected meteorological data (including temperature, evaporation, and precipitation) from 53 meteorological stations in Northeast China from 1999 to 2020. Correlation analysis indicated that the surface water changes have positive correlation with local precipitation. By contrast, the surface water dynamic was weakly related with evaporation and temperature (Table 3). As shown in Fig. 9, precipitation fluctuation is generally consistent with surface water dynamics. Since the turning point in 2001, the annual precipitation has experienced an upward trend. The annual rainfall from 1999–2010 was 480.78 mm, which increased to 582.87 mm from 2011–2020. The intercedes variation of the precipitation increase can explain the overall increased trend of surface water in Northeast China. Under the fluctuating upward trend, the two peaks of surface water area in 2013 and 2020 were mainly related to the flood disasters caused by abnormal precipitation in these two years. In addition to climatic factors, human activities in Northeast China have also impacted the spatial distribution and change trend of surface water. For example, Hulun Lake reached its lowest water level since 1960 in 2012. Since then, through engineering measures of artificial water transfer, the shrinking trend of Hulun Lake has been curbed, and the water level has continued to rise. From 2012 to 2019, the lake water level and volume increased by approximately 2.65 m and 5.18 Gt, respectively (Fan et al., 2021). In addition, the substantial increase in temporary water in Northeast China revealed here was influenced by the 'conversion from dry fields to paddy fields'. As an essential part of the transformation of cultivated land use, the conversion of dry fields to paddy fields has played an active role in regulating the relationship between man and land, increasing grain output, and improving people's lives. The large expansion of paddy fields is also an important reason for this region's increase in surface water area. According to Man et al. (2016), from 2000 to 2013, the average annual growth of paddy field area in Northeast China reached 1078.35 km^2/yr, and the proportion of paddy fields to total cultivated land continually rose. In addition, the newly impounded reservoirs contribute to the surface water expansion, especially in the southern mountain area.

Table 3 Correlation results between meteorological factor and surface water changes

Area	Precipitation	Temperature	Evaporation
Seasonal water area	0.69	0.10	−0.43
Permanent water area	0.55	−0.31	−0.25
Equivalent area	0.77	−0.02	−0.45

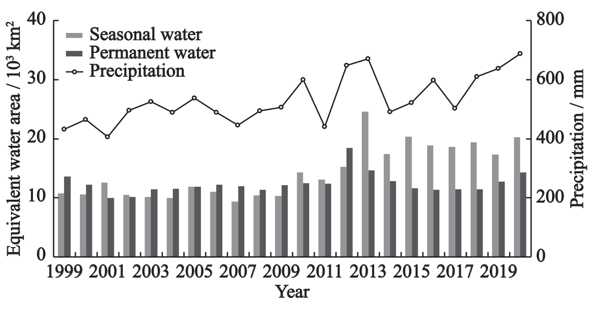

Fig. 9 Annual variation trends of surface water and average precipitation derived from 53 meteorological stations in Northeast China

5 Conclusions

In this study, the global surface water dynamic data GLAD GSWD was selected to track the long-term variability of surface water in Northeast China from 1999–2020. Compared with the previous studies, the refined classification of water bodies in this study can reveal the divergent change patterns of six water body types (e.g., lake, reservoir, river, coastal aquaculture, marsh wetland, ephemeral water). Equivalent water area, which considers the probability of water presence, was used for analyzing spatial-temporal variations at interdecadal and interannual scales.

The results show that surface water in Northeast China was mainly distributed in the central and eastern regions, while seasonal water bodies were primarily distributed along both banks of rivers from 1999–2020. Among all surface water types, ephemeral water bodies have the largest area, accounting for 44.62% of the total surface water area in 2020. In the past two decades, the equivalent surface water area of Northeast China experienced a dramatic increase, ranging from 24 394 to 34 595 km^2. The surge of ephemeral water is the primary contributor of surface water expansion. The annual fluctuation of the permanent water body area was slight, while the seasonal water body area was large. The proportion of seasonal and permanent water bodies changed from 44.14% and 55.86% to 58.67% and 41.33%, respectively. Seasonal water area has gradually become the dominant part of surface water area in Northeast China. Both climate change and human activities contribute to the long-term variation of surface water in Northeast China. The increase in precipitation and the transformation from dry land to paddy fields drive the surface water expansion. In addition, the newly constructed reservoir made a significant contribution, particularly in Northeast China's southern mountain region. The above findings will provide an essential reference for the conservation and efficient utilization of water resources in Northeast China.

Conflict of Interest

The authors declare that they have no known competing financial interests or personal relationships that could have appeared to influence the work reported in this paper.

Author Contributions

All authors contributed to the study conception and design. Material preparation, data collection and analysis were performed by LIU Kai, ZHANG Dapeng and SONG Chunqiao. The first draft of the manuscript was written by LIU Kai and all authors commented on previous versions of the manuscript. All authors read and approved the final manuscript.

Supplementary

Tables S1–S3 and Fig. S1 could be found at http://egeoscien.neigae.ac.cn/article/2024/1.

References

Allen G H, Pavelsky T M, 2018. Global extent of rivers and streams. *Science*, 361(6402): 585–588. doi: 10.1126/science.aat0636

Christian J I, Basara J B, Hunt E D et al., 2021. Global distribution, trends, and drivers of flash drought occurrence. *Nature Communications*, 12(1): 6330. doi: 10.1038/s41467-021-26692-z

Cooley S W, Ryan J C, Smith L C, 2021. Human alteration of global surface water storage variability. *Nature*, 591(7848): 78–81. doi: 10.1038/s41586-021-03262-3

Du B J, Wang Z M, Mao D H et al., 2020. Tracking lake and reservoir changes in the Nenjiang Watershed, Northeast China: patterns, trends, and drivers. *Water*, 12(4): 1108. doi: 10.3390/W12041108

Fan C Y, Song C Q, Liu K et al., 2021. Century-scale reconstruction of water storage changes of the largest lake in the Inner Mongolia Plateau using a machine learning approach. *Water Resources Research*, 57(2): e2020WR028831. doi: 10.1029/2020WR028831

Gao S, Li Z, Chen M Y et al., 2021. Spatiotemporal variability of global river extent and the natural driving factors revealed by decades of Landsat observations, GRACE gravimetry observations, and land surface model simulations. *Remote Sensing of Environment*, 267: 112725. doi: 10.1016/j.rse.2021.112725

Luo S X, Song C Q, Ke L H et al., 2022. Satellite laser altimetry reveals a net water mass gain in Global Lakes with spatial heterogeneity in the early 21st century. *Geophysical Research Letters*, 49(3): e2021GL096676. doi: 10.1029/2021gl096676

Man Weidong, Wang Zongming, Liu Mingyue et al., 2016. Spatio-temporal dynamics analysis of cropland in Northeast China during 1990–2013 based on remote sensing. *Transactions of the Chinese Society of Agricultural Engineering*, 32(7): 1–10. (in Chinese)

Mao D H, Wang Z M, Du B J et al., 2020. National wetland mapping in China: a new product resulting from object-based and hierarchical classification of Landsat 8 OLI images. *ISPRS Journal of Photogrammetry and Remote Sensing*, 164: 11–25. doi: 10.1016/j.isprsjprs.2020.03.020

Messager M L, Lehner B, Grill G et al., 2016. Estimating the volume and age of water stored in global lakes using a geostatistical approach. *Nature Communications*, 7(1): 13603. doi: 10.1038/ncomms13603

Pekel J F, Cottam A, Gorelick N et al., 2016. High-resolution mapping of global surface water and its long-term changes. *Nature*, 540(7633): 418–422. doi: 10.1038/nature20584

Pi X H, Luo Q Q, Feng L et al., 2022. Mapping global lake dynamics reveals the emerging roles of small lakes. *Nature Communications*, 13(1): 5777. doi: 10.1038/s41467-022-33239-3

Pickens A H, Hansen M C, Hancher M et al., 2020. Mapping and sampling to characterize global inland water dynamics from 1999 to 2018 with full Landsat time-series. *Remote Sensing of Environment*, 243: 111792. doi: 10.1016/j.rse.2020.111792

Pickens A H, Hansen M C, Stehman S V et al., 2022. Global seasonal dynamics of inland open water and ice. *Remote Sensing of Environment*, 272: 112963. doi: 10.1016/j.rse.2022.112963

Shan W, Qiu L S, Guo Y et al., 2022. Dynamic analysis in surface water area and its driving factors in Northeast China from 1988 to 2020. *Water*, 14(15): 2296. doi: 10.3390/w14152296

Sheng Y W, Song C Q, Wang J D et al., 2016. Representative lake water extent mapping at continental scales using multitemporal Landsat-8 imagery. *Remote Sensing of Environment*, 185: 129–141. doi: 10.1016/j.rse.2015.12.041

Shugar D H, Burr A, Haritashya U K et al., 2020. Rapid worldwide growth of glacial lakes since 1990. *Nature Climate Change*, 10(10): 939–945. doi: 10.1038/s41558-020-0855-4

Song C Q, Fan C Y, Zhu J Y et al., 2022. A comprehensive geospatial database of nearly 100000 reservoirs in China. *Earth System Science Data*, 14(9): 4017–4034. doi: 10.5194/essd-14-4017-2022

Tulbure M G, Broich M, Stehman S V, 2016. Spatiotemporal dynamics of Surface water extent from three decades of seasonally continuous Landsat time series at subcontinental scale. In: *The International Archives of the Photogrammetry, Remote Sensing and Spatial Information Sciences*. Prague, Czech Republic: ISPRS, 403–404. doi: 10.5194/isprsarchives-XLI-B8-403-2016

Wang J D, Walter B A, Yao F F et al., 2021. GeoDAR: Georeferenced global dam and reservoir dataset for bridging attributes and geolocations. *Earth System Science Data*, 14: 1869–1899. doi: 10.5194/essd-14-1869-2022

Wang Y, Zhou L, Ping X Y et al., 2018. Ten-year variability and environmental controls of ecosystem water use efficiency in a rainfed maize cropland in Northeast China. *Field Crops Research*, 226: 48–55. doi: 10.1016/j.fcr.2018.07.006

Wang Z M, Mao D H, Li L et al., 2015. Quantifying changes in multiple ecosystem services during 1992–2012 in the Sanjiang Plain of China. *Science of The Total Environment*, 514: 119–130. doi: 10.1016/j.scitotenv.2015.01.007

Weekley D, Li X G, 2019. Tracking multidecadal lake water dynamics with landsat imagery and topography/bathymetry. *Water Resources Research*, 55(11): 8350–8367. doi: 10.1029/2019WR025500

Xu Y Y, Cheng X, Gun Z, 2022. What drive regional changes in the number and surface area of lakes across the Yangtze River basin during 2000–2019: human or climatic factors? *Water Resources Research*, 58(2): e2021WR030616. doi: 10.1029/2021wr030616

Yan F Q, Zhang S W, 2019. Ecosystem service decline in response to wetland loss in the Sanjiang Plain, Northeast China. *Ecological Engineerting*, 130: 117–121. doi: 10.1016/j.ecoleng.2019.02.009

Yang K H, Yao F F, Wang J D et al., 2017. Recent dynamics of alpine lakes on the endorheic Changtang Plateau from multimission satellite data. *Journal of Hydrology*, 552: 633–645. doi: 10.1016/j.jhydrol.2017.07.024

Yu Xiaofei, Ding Shanshan, Zou Yuanchun et al., 2018. Review of rapid transformation of floodplain wetlands in Northeast China: roles of human development and global environmental change. *Chinese Geographical Science*, 28(4): 654–664. doi: 10.1007/s11769-018-0957-3

Zhang G Q, Yao T D, Chen W F et al., 2019a. Regional differences of lake evolution across China during 1960s–2015 and its natural and anthropogenic causes. *Remote Sensing of Environment*, 221: 386–404. doi: 10.1016/j.rse.2018.11.038

Zhang W S, Song C Q. 2022. Spatial distribution and dynamics of lakes in China: progress in remote sensing monitoring at national scale and new inventory of the maximum lake extent and change trajectory. *National Remote Sensing Bulletin*, 26(1): 92–103. (in Chinese)

Zhang X, Liu L Y, Chen X D et al., 2021. GLC_FCS30: global land-cover product with fine classification system at 30 m using time-series Landsat imagery. *Earth System Science Data*, 13(6): 2753–2776. doi: 10.5194/essd-13-2753-2021

Zhang Y, Zang S Y, Sun L et al., 2019b. Characterizing the changing environment of cropland in the Songnen Plain, Northeast China, from 1990 to 2015. *Journal of Geographical Sciences*, 29(5): 658–674. doi: 10.1007/s11442-019-1620-3

Zhang Y L, Deng J M, Qin B Q et al., 2023. Importance and vulnerability of lakes and reservoirs supporting drinking water in China. *Fundamental Research*, 3(2): 265–273. doi: 10.1016/j.fmre.2022.01.035

Zhou Y, Dong J W, Xiao X M et al., 2019. Continuous monitoring of lake dynamics on the Mongolian Plateau using all available Landsat imagery and Google Earth Engine. *Science of the Total Environment*, 689: 366–380. doi: 10.1016/j.scitotenv.2019.06.341

Zhou Y, Dong J W, Cui Y P et al., 2022. Rapid surface water expansion due to increasing artificial reservoirs and aquaculture ponds in North China Plain. *Journal of Hydrology*, 608: 127637. doi: 10.1016/j.jhydrol.2022.127637

Zou Z H, Dong J W, Menarguez M A et al., 2017. Continued decrease of open surface water body area in Oklahoma during 1984–2015. *Science of the Total Environment*, 595: 451–460. doi: 10.1016/j.scitotenv.2017.03.259